Fitoterapia 105 (2015) 177–186

Contents lists available at ScienceDirect

Fitoterapia

journal homepage: www.elsevier.com/locate/fitote

Metabolism of Chuanxiong Rhizoma decoction: Identification of the metabolites in WZS-miniature pig urine

Lei Zhang, Dong-Hui Yang *, Xin Zhao, Feng Xu, Jing Liang, Qi-Le Zhou, Xiao-Yan Yang, Xiu-Wei Yang *

Department of Natural Medicines, School of Pharmaceutical Sciences, Peking University, Beijing 100191, PR China

ARTICLE INFO

Article history:
Received 3 May 2015
Received in revised form 28 June 2015
Accepted 1 July 2015
Available online 7 July 2015

Keywords:
Ligusticum chuanxiong
Phthalides
Phenolic acids
Metabolites *in vivo*
WZS-miniature pig

ABSTRACT

Chuanxiong Rhizoma (CR), a well-known traditional Chinese medicine originated from the rhizome of *Ligusticum chuanxiong* Hort., was effective for treating various vascular diseases. To identify the metabolites of CR *in vivo*, the drug-containing urine samples of WZS-miniature pigs after orally administrated CR decoction were collected, after sequential column chromatography 17 metabolites (**M1**–**M17**) were isolated from the methanol extract of the urine samples. Their structures, including nine phthalides (**M1**–**M9**) and eight phenolic acids (**M10**–**M17**), were identified by spectroscopic means. Among them, 8 were new ones (**M1**–**M6**, **M11**–**M12**). On the basis of the structures of identified metabolites, seven original constituents, including 2 phthalides (senkyunolideI/H) and 5 phenolic acids (ferulic acid, isoferulic acid, caffeic acid, 3-hydroxycinnamoyl acid and 4-hydroxybenzonic acid) were deduced to be the major absorbed original constituents of CR *in vivo*. This is the first study on the metabolites of CR decoction in non-rodent animal (WZS-miniature pig), the results will give an insight into the metabolism profiles of phthalides and phenolic acids in CR decoction *in vivo*.

1. Introduction

Chuanxiong Rhizoma (CR), the rhizome of *Ligusticum chuanxiong* Hort. (Chuanxiong), is a well-known traditional Chinese medicine that is commonly prescribed for the treatment of migraine and various cardiovascular diseases, such as angina pectoris and ischemic stroke [1–3] and endocrine disorders [4] in clinical practice.

To date, a lot of chemical constituents have been isolated from CR, mainly including two types of phthalides (ligustilide, senkyunolide A-S, butylidenephthalide, and phthalide dimers, etc.) [5–9] and phenolic acids (ferulic acid, isoferulic acid and caffeic acid, etc.) [10], and alkaloids (tetramethylpyrazine) [11]. However, which were responsible for CR activities are still uncertain.

Generally, a traditional Chinese medicine (TCM) is administered in the form of decoction, there usually have multiple components. As known, only the absorbed constituents have the most possibilities for being its effective constituents, so, it is important to understand the absorptive constituents of a TCM and their *in vivo* metabolite profiles. To the best of our knowledge, there were much research on the metabolites of the pure compounds in CR, and more than 30 *in vivo* metabolites, which originated from Z-ligustilide, butylphthalide, butylidenephthalide, ferulic acid, caffeic acid and tetramethylpyrazine, have been identified mainly by analyzing their MS information, respectively [12–26]. There was only one report on the overall metabolism of CR extract in rat's plasma [27], which led to the identification of 13 prototype constituents and 12 conjugated metabolites basing on HPLC–MS information.

In the present study, the CR metabolites existed in the drug-containing urine samples of WZS-miniature pigs after orally administrated CR decoction, were isolated using a series of column chromatographies, which led to 17 compounds, and their structures were elucidated on the basis of MS and spectroscopic analyses.

2. Materials and methods

2.1. Materials

The CR materials were purchased from Yaoxing Medicinal Materials Company (Anguo, Hebei Province, China) and were identified as the dried rhizome of *Ligusticum chuanxiong* Hort. (Umbelliferae) by D.-H. Yang. The voucher specimen (No. 6332) was deposited in Herbarium of Pharmacognosy, School of Pharmaceutical Sciences, Peking University. The dry powders of CR crude drugs (15 kg) were immersed in 150 L of water for 1 h, and then decocted for 1.5 h. After filtration, the residue was decocted again with 90 L of water for 1 h. The two filtered extracts were combined and concentrated to about 7 L (2.14 g crude drug/mL) by rotatory evaporation *in vacuum* at 60 °C and stored at −20 °C before use.

* Corresponding authors at: No. 38, Xueyuan Road, Haidian District, Beijing 100191, PR China.
E-mail addresses: ydhui@bjmu.edu.cn (D.-H. Yang), xwyang@bjmu.edu.cn (X.-W. Yang).

http://dx.doi.org/10.1016/j.fitote.2015.07.001
0367-326X/

2.2. Chemicals and reagents

HPLC-grade acetonitrile and methanol were purchased from Fisher Scientific (Fairlawn, NJ, USA) and Tianjin Damao Chemical Company (Tianjin, China). Analytical-grade formic acid was purchased from MREDA Technology (USA). Purified water was prepared by a Milli-Q water purification system (Millipore, Bedford, MA, USA). Analytical-grade methanol and ethanol were provided by Peking Chemical Factory (Beijing, China). XAD-2 macroporous resin (Amberlite, Philadelphia, USA) and Sephadex LH-20 (GE health care, Buckinghamshire, UK) were used for isolation.

2.3. Animal protocol

Eight male WZS-miniature pigs (each weighing about 60 kg) were purchased from the Institute of Animal Science, Chinese Academy of Agricultural Sciences. The pigs were raised in metabolic cages in an environmentally controlled room (25 °C and 60% relative humidity) for consecutive 7 days before the experiment. Each pig was orally administered with 125 mL of distilled water (twice per day, 8:00 a.m. and 5:00 p.m.) in the first 2 days for collecting the blank urine sample. Then an equal dose (125 mL, 5.4 g crude drug/kg) of the CR decoction (twice per day, 8:00 a.m. and 5:00 p.m.) was administered in the followed 4 days, and the drug-containing urine samples were collected since the first administration.

All the procedures were in strict accordance with the guidelines for Animal Experimentation of Peking University (Beijing, China), and the protocols were approved by the Animal Biomedical Ethical Committee of Peking University (Approval No. LA2011-058).

2.4. Urine samples

Prior to the drug administration, the blank urine sample within 48 h (40 L) was collected; then the drug-containing urine samples were continuously collected until 12 h after the last administration, 95% ethanol as preservative was added into the urine samples (100 mL/L) during collection. The urine sample (approximately 20 L/day) was filtered through absorbent cotton, and equal amount of methanol was added into the urine sample to precipitate endogenous protein and carbamide. After vacuum suction filtration, the filtrate was evaporated in vacuum at 50 °C to obtain the drug-containing urine extract (1.12 kg), which was stored at −20 °C before further isolation. Blank urine sample was pre-treated by the same procedure.

2.5. Extraction and isolation

The drug-containing urine extract (1.10 kg) was dissolved in 1 L of distilled water, and then chromatographed on a XAD-2 macroporous resin column (5 kg, 2 × 30 cm) using gradient elution of methanol–water solutions, which gave 3 fractions of Fr.1 (eluted by water), Fr.2 (eluted by 20% methanol), and Fr.3 (eluted by 50% methanol). By analyzing their HPLCs, the major constituents originating from CR decoction were detected in Fr. 2 and Fr. 3, while Fr. 1 was mainly composed of endogenous components (Fig. 1). Therefore, Fr. 2 and Fr. 3 were merged for the following chemical isolation, and 17 compounds (**M1**–**M17**) were isolated after consecutive column separations on semi-preparative HPLC and Sephadex LH-20.

2.6. Equipment and chromatographic conditions

The HPLC chromatography system consisted of Shimadzu LC-20A pumps, a SPD-M20A PDA detector (Shimadzu, Japan), and a Phenomenex ODS column (250 × 4.6 mm, 5 μm; Phenomenex, Inc.), developed with a linear gradient from 3% to 60% CH_3CN/H_2O (containing 0.3% trifluoroacetic acid) in 95 min followed by additional 5 min elution with 100% CH_3CN at a flow rate of 1.0 mL/min and UV detection elution with 280 nm.

Semi-preparative HPLC chromatography system consisted of Agilent 1100 pumps equipped with an DAD detector (Agilent Co.) and a Phenomenex ODS column (250 × 21.2 mm, 10 μm; Phenomenex, Inc.), using CH_3CN-H_2O (containing 0.3% trifluoroacetic acid) as eluent at a flow rate of 3 mL/min.

MS data of the isolated compounds were measured on Waters Xevo G2-S QT of mass spectrometer. The IR absorption spectra were obtained on a JASCO IR-810 spectrophotometer. Circular dichroism (CD) and induced CD spectra were taken on a JASCO J-810 spectro polarimeter (JASCO Co.).

NMR spectra were performed in an inverse probe of Bruker-AVIII-500 and Bruker-AVIII-500 spectrometer with TMS as the internal standard, and coupling constants (*J* values) were given in Hertz.

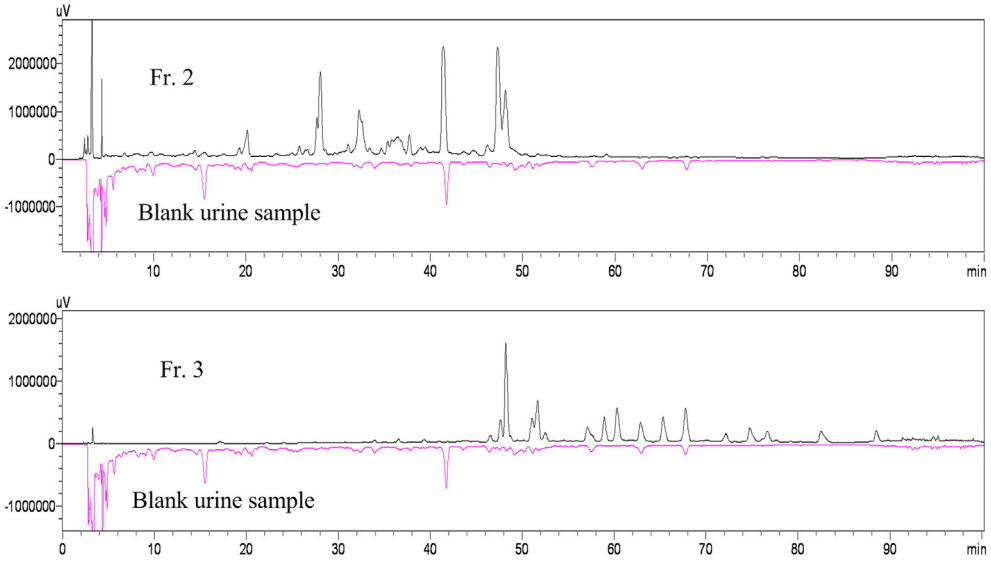

Fig. 1. The HPLCs of blank urine sample and fractions of drug-containing urine samples from XAD-2 resin column chromatography eluted by 20% methanol (Fr.2) and 50% methanol (Fr.3), respectively.

2.7. Data of the compounds (*M1*–*M17*)

M1, slight yellow solid, HR–ESI–MS m/z 263.0894 $[M + Na]^+$ (calcd for $C_{12}H_{16}O_5Na^+$: m/z 263.0895); IR (KBr) ν_{max} 3391.24 (–OH), 1748.3, 1677.8, 1202.6 and 1039.7 (C═O) cm^{-1}. The NMR data were shown in Table 1.

M2, slight yellow solid, HR–ESI–MS m/z 263.0896 $[M + Na]^+$ (calcd for $C_{12}H_{16}O_5Na^+$: m/z 263.0895), IR (KBr) ν_{max} 3401.6 (–OH), 1749.4, 1677.2 and 1203.5 (C═O) cm^{-1}. The NMR data were shown in Table 1.

M3, slight yellow solid, HR–ESI–MS m/z 263.0892 $[M + Na]^+$ (calcd for $C_{12}H_{16}O_5Na^+$: 263.0895), IR (KBr) ν_{max} 3420.0 (–OH), 1749.4, 1654.9, 1026.3 and 1002.2 (C═O) cm^{-1}. The NMR data were shown in Table 1.

M4, slight yellow solid, HR–ESI–MS m/z 253.0715 $[M–H]^-$ (calcd for $C_{12}H_{13}O_6^-$: m/z 253.0712), IR (KBr) ν_{max} 3415.1 (–OH), 1750.2, 1680.0, 1202.8 and 1032.6 (C═O) cm^{-1}. The NMR data were shown in Table 2.

M5, slight yellow solid, HR–ESI–MS m/z 253.0721 $[M–H]^-$ (calcd for $C_{12}H_{13}O_6^+$: m/z 253.0712), IR (KBr) ν_{max} 3401.9 (–OH), 1677.2, 1201.9 and 1116.3 (C═O) cm^{-1}. The NMR data were shown in Table 2.

M6, slight yellow solid, HR–ESI–MS m/z 291.0848 $[M + Na]^+$ (calcd for $C_{13}H_{16}O_6Na^+$: m/z 291.0845), IR (KBr) ν_{max} 3401.9 (–OH), 1677.2, 1201.9 and 1116.3 (C═O) cm^{-1}. The NMR data were shown in Table 2.

M7, slight yellow solid, HR–ESI–MS m/z 399.1294 $[M–H]^-$ (calcd for $C_{18}H_{23}O_{10}^-$: m/z 399.1291), IR (KBr) ν_{max} 3395.4 (–OH), 1742.8, 1676.3, 1260.4, 1112.6 and 1041.0 (C═O) cm^{-1}. The NMR data were shown in Table 3.

M8, slight yellow solid, HR–ESI–MS m/z 399.1287 $[M–H]^-$ (calcd for $C_{18}H_{23}O_{10}^-$: m/z 399.1291), IR (KBr) ν_{max} 3395.4 (–OH), 1742.8, 1676.3, 1260.4, 1112.6 and 1041.0 (C═O) cm^{-1}. The NMR data were shown in Table 3.

M9, slight yellow solid, HR–ESI–MS m/z 399.1284 $[M–H]^-$ (calcd for $C_{18}H_{23}O_{10}^-$: m/z 399.1291), IR (KBr) ν_{max} 3395.4 (–OH), 1742.8, 1676.3, 1260.4, 1112.6 and 1041.0 (C═O) cm^{-1}. The NMR data were shown in Table 3.

M10, slight yellow solid, ESI–MS m/z 252.08 $[M–H]^-$ (calcd for $C_{12}H_{14}NO_5^-$: m/z 252.0877). The NMR data were shown in Tables 4 and 5.

M11, slight yellow solid, HR–ESI–MS m/z 260.0896 $[M + Na]^+$ (calcd for $C_{12}H_{15}NO_4Na^+$: m/z 260.0899), IR (KBr) ν_{max} 3403.9 (–NH–), 1740.3, 1648.5, 1234.2 and 1024.9 (C═O) cm^{-1}. The NMR data were shown in Tables 4 and 5.

M12, slight yellow solid, HR–ESI–MS m/z 266.0664 $[M–H]^-$ (calcd for $C_{12}H_{12}NO_6^-$: m/z 266.0670), IR (KBr) ν_{max} 3395.4 (–OH), 1742.8, 1676.3, 1260.4, 1112.6 and 1041.0 (C═O) cm^{-1}. The NMR data were shown in Tables 4 and 5.

M13, slight yellow solid, HR–ESI–MS m/z 250.0720 $[M–H]^-$ (calcd for $C_{12}H_{12}NO_5^-$: m/z 250.0715). The NMR data were shown in Tables 4 and 5.

M14, slight yellow solid, HR–ESI–MS m/z 264.0878 $[M–H]^-$ (calcd for $C_{13}H_{14}NO_5^-$: m/z 264.0872). The NMR data were shown in Tables 4 and 5.

M15, slight yellow solid, ESI–MS m/z 242.13 $[M + Na]^+$ (calcd for $C_{12}H_{13}NO_3Na^+$: m/z 242.0788). The NMR data were shown in Tables 4 and 5.

M16, slight yellow solid, ^1H NMR (400 MHz, DMSO) δ: 7.21 (1H, t, J = 8.0, 7.6 Hz, H-3), 7.09 (1H, d, J = 7.6 Hz, H-5′), 7.03 (1H, s, H-6′), 6.83 (1H, d, J = 8 Hz, H-2′), 7.48 (1H, d, J = 15.6 Hz, H-4′), 6.42 (1H, d, J = 16 Hz, H-2). ^{13}C NMR (100 MHz, DMSO) δ: 167.6 (C-1), 157.6 (C-3′), 143.9 (C-3), 135.5 (C-1′), 129.8 (C-5′), 119.1 (C-6′), 119.1 (C-2), 117.3 (C-2′), 114.4 (C-4′).

M17, slight yellow solid, ^1H NMR (400 MHz, DMSO) δ: 12.48 (1H, s, –COOH), 10.32 (1H, s, —OH), 7.79 (2H, d, J = 8 Hz, H-2,6), 6.82 (2H, d, J = 8.6 Hz, H-3,5). ^{13}C NMR (100 MHz, DMSO) δ: 167.6 (–COOH), 162.1 (C-1), 132.0 (C-3,5), 121.8 (C-4), 115.6 (C-2,6).

3. Results and discussion

3.1. Structure elucidation

The identified 17 compounds (**M1**–**M17**), including nine phthalide-related compounds (**M1**–**M9**) and eight phenolic acid-related compounds (**M10**–**M17**), were determined on the basis of their spectroscopic data (Fig. 2). Their chemical structures were identified as: *Z-(6S,7R,10R)*-3-butylidene-4,5,6,7-tetrahydro-6,7,10-trihydroxyphthalide (**M1**), *Z-(6S,7R,10S)*-3-butylidene-4,5,6,7-tetrahydro-6,7,10-trihydroxyphthalide (**M2**), *Z-(6R,7S)*-3-butylidene-4,5,6,7-tetrahydro-6,7,10-trihydroxyphthalide (**M3**), *E-(6S,7R)*-3-butylidene-4,5,6,7-tetrahydro-11-carboxylic-6,7-dihydroxyphthalide (**M4**), *Z-(6S,7R)*-3-butylidene-4,5,6,7-tetrahydro-11-carboxylic-6,7-dihydroxyphthalide (**M5**), *(6S,7R)*-3-butylidene-4,5,6,7-tetrahydro-11-carboxylic-6,7-dihydroxyphthalide-11-methyl ether (**M6**), *Z-(6S,7R)*-3-butylidene-4,5,6,7-tetrahydro-6,7-dihydroxyphthalide-7-*O*-β-D-glucuronide (**M7**), *E-(6S,7R)*-3-butylidene-4,5,6,7-tetrahydro-6,7-dihydroxyphthalide-6-*O*-β-D-glucuronide (**M8**), *E-(6S,7R)*-3-butylidene-4,5,6,7-tetrahydro-6,7-dihydroxyphthalide-7-*O*-β-D-glucuronide (**M9**), *N*-(4,5-dihydro-feruoyl)-glycine (**M10**), *N*-(3′-hydroxy-4,5-dihydro-cinnamoyl)-glycine-methyl ether (**M11**), *N*-(4,5-dihydro-5-carbonyl-feruoyl)-glycine (**M12**), *N*-(3′-hydroxy-4′-methoxy-cinnamoyl)-glycine (**M13**), *N*-(3′,4′-dimethoxy-cinnamoyl)-glycine (**M14**), *N*-cinnamoyl-glycine-methyl ether (**M15**), *trans*-3-hydroxycinnamoyl acid (**M16**), and 4-hydroxybenzoic acid (**M17**).

Among them, eight compounds (**M1**–**M6**, **M11**–**M12**) are new ones, and the other 9 known compounds were first isolated as absorptive

Table 1
^1H NMR (δ) and ^{13}C NMR data (δ) for **M1**, **M2** and **M3** in MeOD, δ in ppm, J in Hz[a].

No.	δ_H				δ_C			
	Senkyunolide R	M1	M2	M3	Senkyunolide R	M1	M2	M3
1					170.25	169.3	169.3	168.7
3					149.1	149.3	149.3	149.1
3a					155.5	153.9	153.8	153.9
4	2.47–2.63 (2H, m)	2.50–2.58 (2H, m)	2.56–2.61 (2H, m)	2.55–2.73 (1H, m, 4a) 2.53–2.55 (1H, m, 4b)	18.21	16.8	16.8	19.5
5	1.89–2.03 (2H, m)	1.92–2.00 (2H, m)	1.95–2.05 (2H, m)	1.98–2.03 (1H, m) 1.84–1.88 (1H, m)	25.08	23.7	23.7	24.2
6	3.96 (1H, ddd, 5.4, 3.4, 2.4)	3.97 (1H, d, 2.4)	3.99 (1H, s)	3.81 (1H, dt, 11, 3.5)	71.02	69.6	69.6	69.0
7	4.25 (1H, d, 3.4)	4.27 (1H, d, 3.6)	4.29 (1H, d, 2.4)	4.45 (1H, d, 3.5)	65.44	64.0	64.0	61.8
7 a					127.8	125.4	125.4	126.6
8	5.35 (1H, d, 8.8)	5.53 (1H, t, 8.0)	5.55 (1H, t, 7.8)	5.53 (1H, t, 8.0)	115.70	109.4	109.4	109.6
9	4.61 (1H, dt, 8.8, 6.4)	2.42–2.47 (2H, m)	2.53–2.55 (2H, m)	2.53–2.55 (2H, m)	68.69	35.2	35.1	35.1
10	1.52–1.63 (1H, m)							
	1.64–1.75 (1H, m)	3.92 (1H, q, 6.4)	3.94 (1H, q, 6.0)	3.92 (1H, q, 6.0)	31.16	66.5	66.5	66.4
11	0.94 (3H, t, 7.3)	1.22 (3H, d, 6.5)	1.23 (3H, d, 6.6)	1.22 (3H, d, 6.0)	9.96	21.8	21.8	21.8

[a] ^{13}C NMR data (δ) were measured at 125 MHz for **M1**–**M3**. ^1H NMR data (δ) were measured at 500 MHz for **M1**–**M3**.

Table 2
^{1}H NMR (δ) and ^{13}C NMR data (δ) for **M4**, **M5** and **M6** in MeOD, δ in ppm, J in Hz[a].

No.	δ_H				δ_C			
	Senkyunolide H	**M4**	**M5**	**M6**	Senkyunolide H	**M4**	**M5**	**M6**
1					169.2	169.1	168.5	169.3
3					148.5	148.7	148.6	149.2
3a					153.0	153.9	153.9	154.0
4	2.36–2.42 (1H, m) 2.62–2.69 (1H, m)	2.50–2.56 (2H, m)	2.58–2.69 (1H, m) 2.46–2.54 (1H, m)	2.52–2.55 (2H, m)	19.1	16.8	19.5	16.7
5	1.79–1.85 (1H, m) 2.10–2.17 (1H, m)	1.92–1.99 (2H, m)	1.96–2.02 (1H, m) 1.84–1.89 (1H, m)	1.91–2.02 (2H, m)	26.7	23.7	24.2	23.6
6	4.06 (1H, ddd, 7.9, 3.9, 2.5)	3.96 (1H, d, 2.5)	3.79 (1H, dt, 3.5, 5.0)	3.79 (1H, q, 3.5)	71.9	69.7	68.9	69.6
7	4.61 (1H, d, 3.9)	4.27 (1H, d, 3.0)	4.44 (1H, d, 3.0)	4.27 (1H, d, 2.5)	68.0	64.0	61.7	64.0
7a					126.3	125.5	126.7	128.3
8	5.31 (1H, t, 7.9)	5.50 (1H, t, 7.5)	5.48 (1H, t, 7.5)	5.48 (1H, t, 7.5)	114.1	111.0	111.2	111.6
9	2.36 (2H, dt, 7.9, 7.4)	2.68–2.63 (2H, m)	2.58–2.69 (2H, m)	2.65–2.69 (2H, q, 7)	28.2	21.2	21.2	21.1
10	1.50 (2H, tq, 7.4, 7.4)	2.63–2.68 (1H, m) 2.50–2.56 (1H, m)	2.46–2.54 (2H, m)	2.57–2.59 (2H, m)	22.4	32.4	32.5	32.4
11	0.95 (3H, t, 7.4)				13.7	174.8	175.5	175.1
12				3.69 (3H, s)				50.9

[a] ^{13}C NMR data (δ) were measured at 125 MHz for **M4**–**M6**. ^{1}H NMR data (δ) were measured at 500 MHz for **M4**–**M6**.

constituents or metabolites of the CR decoction *in vivo*, the NMR data of 7 known compounds (**M7**–**M9**, **M10**, **M13**–**M15**) are reported here for the first time.

M1–**M3** showed the molecular formula of $C_{12}H_{16}O_5$ in HRESI–MS, and UV λ_{max} at 280 nm. ^{1}H NMR and ^{13}C NMR spectra of them were similar to senkyunolide R ($C_{12}H_{16}O_5$) [7], except for the branched chain signals at C-8, C-9, C-10 and C-11 (Table 1), which suggested that **M1**–**M3** should be similar to senkyunolide R. Basing on the 4 proton signals in the branched chain of **M1**–**M3** at δ 5.53/5.55/5.53 (H-8, 1H, t, J = 8.0 Hz), 2.42/2.53/2.53 (H-9, 2H, m), 3.92/3.94/3.92 (H-10, 1H, q, J = 6.4 Hz) and 1.22/1.23/1.22 (H-11, 3H, d, J = 6.5 Hz), it was suggested that one hydroxyl group was attached to C-10 (δ 66.5/66.5/66.4) [5,6], which could be proved by the correlations of H8/H9, H9/H10, H10/H11 in ^{1}H–^{1}H COSY spectrum, as well as the correlations between H-9 and C-3 (δ 149.3/149.3/149.1) in HMBC spectrum (Fig. 3). Thus, the planar structure of **M1**–**M3** was deduced as *3*-butylidene-4,5,6,7-tetrahydro-6,7,10-trihydroxyphthalide. There were three chiral centers (C-6, C-7, and C-10) and one double bond (Δ3,8) in **M1**–**M3**. The relative configuration of the 6,7-dihydroxy groups was deduced to be in *cis* basing on the $J_{6,7}$ value of 3.6 Hz which was similar to that ($J_{6,7}$ = 3.9 Hz) of senkyunolide H [5,7], as well as the NOESY correlation between H-6 (δ3.97/3.99/3.81) and H-7 (δ4.27/4.29/4.45) (Fig. 4). The NOE effect for H-4 (δ2.5, 2H, m) upon irradiation at H-8 (δ5.5, 1H, t, 8.0 Hz) in **M1**–**M3** indicated the Δ3,8-configuration was in *trans*. The absolute configurations at C-6 (δ69.6/69.6/69.0) and C-7 (δ64.0/64.0/61.8) were determined by induced CD spectra after adding $Mo_2(AcO)_4$ (ligand-to-metal ratio: 0.6/0.8) in DMSO (Fig. 5), the 6*S*- and 7*R*-configurations in both **M1** and **M2** were determined due to the positive Cotton effect at 305–310 nm [29], whereas the 6*R*- and 7*S*-configuration in **M3** due to its negative Cotton effect at 305–310 nm. The absolute configuration at C-10 in **M1** and **M2** were identified by adding metal chelating agent $Rh_2(OCOCF_3)_4$. To eliminate the interference of 6,7-dihydroxy groups, the acetonide on C-6 and C-7 of **M1** and **M2** were synthesized to obtain two compounds of **M1a** and **M2a**, and then their induced CD spectra were detected after adding $Rh_2(OCOCF_3)_4$ (ligand-to-metal ratio: 0.6/0.8) in $CHCl_3$. Basing on the positive Cotton effect at 350 nm in the induced CD spectrum of **M1a** [30,31] and negative Cotton effect at 350 nm in **M2a**, 10*R*-configuration in **M1** and 10*S*-configuration in **M2** were determined. In conclusion, the structures of **M1**–**M3** were established as *Z-(6S,7R,10R)*-3-butylidene-4,5,6,7-tetrahydro-6,7,10-trihydroxyphthalide (**M1**), *Z-(6S,7R,10S)*-3-butylidene-4,5,6,7-tetrahydro-6,7,10-trihydroxyphthalide (**M2**), and *Z-(6R,7S)*-3-butylidene-4,5,6,7-tetrahydro-6,7,10-trihydroxyphthalide (**M3**), respectively.

Table 3
^{1}H NMR (δ) and ^{13}C NMR data (δ) for **M7**, **M8** and **M9** in MeOD, δ in ppm, J in Hz[a].

No.	δ_H			δ_C		
	M7	M8	M9	M7	M8	M9
1				169.9	168.2	169.0
3				148.7	147.9	148.1
3a				154.5	153.3	155.0
4	2.55–2.57 (2H, m)	2.40–2.44 (2H, m)	2.49 (2H)	16.3	16.8	17.4
5	1.94–2.0 (1H, m) 2.03–2.21 (1H, m)	1.84–1.86 (1H, m) 1.90–1.93 (1H, m)	1.82 (2H, s)	23.1	22.0	22.8
6	4.27 (1H, s)	3.88 (1H, s)	4.00 (1H, d, 4)	66.4	77.6	66.2
7	4.38 (1H, d, 2.0)	4.25 (1H, s)	4.24 (1H, d, 4)	70.9	60.5	69.2
7a				123.5	125.3	123.1
8	5.50 (1H, t, 8)	5.48 (1H, t, 8)	5.56 (1H, t, 8)	113.4	112.3	113.3
9	2.37 (2H, q, 7.5)	2.26 (2H, q, 8)	2.29 (2H, q, 8)	27.7	27.5	27.6
10	1.55 (2H, q, 7.5)	1.46 (2H, q, 8)	1.46 (2H, q, 8)	21.9	21.7	21.7
11	0.99 (3H, t, 7.5)	0.91 (3H, t, 8)	0.92 (3H, t, 8)	12.7	13.7	13.7
1′	4.68 (1H, d, 7.5)	4.39 (1H, d, 8)	4.48 (1H, d, 8)	102.6	103.0	102.4
2′	3.25 (1H, t, 7.5)	2.88 (1H, t, 8)	2.92 (1H, t, 8)	73.0	73.0	73.1
3′	3.42 (1H, t, 9)	3.15 (1H, t, 8)	3.15 (1H, t, 8)	76.3	75.9	75.9
4′	3.47 (1H, t, 10)	3.28 (1H, t, 8)	3.30 (1H, t, 8)	71.8	71.4	71.5
5′	3.77 (1H, d, 9.5)	3.65 (1H, d, 8)	3.63 (1H, d, 8)	75.0	75.7	75.8
6′				169.9	170.2	170.2

[a] ^{13}C NMR data (δ) were measured at 125 MHz for **M7** and at 100 MHz for **M8**–**M9**. ^{1}H NMR data (δ) were measured at 500 MHz for **M7** and at 400 MHz for **M8**–**M9**.

Table 4
^{1}H NMR (δ) for **M10**–**M15** in DMSO (**M11** and **M14** were in MeOD), δ in ppm, J in Hz[a].

No.	M10	M11	M12	M13	M14	M15
2	3.99 (2H, s)	3.89 (2H, s)	3.79 (2H, d, 4)	3.85 (2H, d, 4.5)	3.87 (2H, d, 5.6)	3.98 (2H, d, 5.6)
4	2.53 (2H, t, 15.5)	2.50 (2H, t, 6.5)	3.87 (2H, s)	6.55 (1H, d, 15.5)	6.60 (1H, d, 16)	6.72 (1H, d, 13.2)
5	2.87 (2H, t, 15.5)	2.84 (2H, t, 7.5)		7.34 (1H, d, 15.5)	7.38 (1H, d, 15.6)	7.46 (1H, d, 13.2)
2′	6.86 (1H, s)	6.64 (1H, s)	7.45 (1H, s)	7.15 (1H, d, 2)	7.18 (1H, s)	7.60 (1H, s)
3′						7.42–7.38 (3H, m)
4′		6.59 (1H, d, 8)				
5′	6.71 (1H, d, 8)	7.06 (1H, t, 7.5)	6.85 (1H, d, 8)	6.80 (1H, d, 8)	6.99 (1H, d, 8.2)	
6′	6.66 (1H, d, 8)	6.67 (1H, d, 7.5)	7.52 (1H, d, 8)	7.01 (1H, d, 8.5)	7.13 (1H, d, 8.2)	7.58 (1H, s)
1-OCH_3		3.68 (3H, s)				3.65 (3H, s)
3′-OCH_3	3.85 (3H, s)		3.81 (3H, s)		3.78 (3H, s)	
4′-OCH_3				3.85 (3H, s)	3.80 (3H, s)	
CO–NH–	8.18 (1H, s)		8.45 (1H, t, 5.5)	8.07 (1H, s)	8.27 (1H, s)	8.55 (1H, s)

[a] ^{1}H NMR data (δ) were measured at 500 MHz for **M10** and at 400 MHz for **M11**–**M15**.

M4 and **M5** showed the same molecular formula of $C_{12}H_{14}O_6$ and the UVλ_{max} at 280 nm. The ^{1}H NMR and ^{13}C NMR data (Table 2) were similar to those of senkyunolide H ($C_{12}H_{16}O_4$), except for the signals at C-9, C-10 and C-11 [5,6]. In place of the methyl signals at δ13.7 (C-11) in senkyunolide H, there is one carboxyl signal at δ 174.8 (**M4**)/175.5 (**M5**). The correlation between H-10 (δ2.63/2.46) and C-11 (δ 174.8/175.5) in HMBC spectra of M4/M5, indicated that the carboxyl group was attached to at C-10 (Fig. 3). Thus, the planar structure of **M4** and **M5** were deduced as 3-butylidene-4,5,6,7-tetrahydro-11-carboxylic-6,7-dihydroxyphthalide. There were also two chiral centers at C-6 and C-7 and one double bond (Δ3,8) in the structures of **M4** and **M5**. The J values of the vicinal coupling between H-6 and H-7 were 3.0 Hz in **M4** and **M5**, indicating that the relative configuration at C-6 and C-7 was in *cis* [5,7]. Based on the positive Cotton effect at 305 nm in the induced CD spectrum of **M4** and **M5**, the absolute configuration of C-6,7 was established as 6*S*,7*R* [29] (Fig. 5). The NOE effect for H-4 upon irradiation at H-8 in **M5** suggested the 3,8-*trans* configuration. Therefore, the structure of **M4** was identified as *E-(6S,7R)*-3-butylidene-4,5,6,7-tetrahydro-11-carboxylic-6,7-dihydroxyphthalide; **M5** was elucidated as *Z-(6S,7R)*-3-butylidene-4,5,6,7-tetrahydro-11-carboxylic-6,7-dihydroxyphthalide.

M6 showed the molecular formula of $C_{13}H_{16}O_6$. The UV, ^{1}H NMR and ^{13}C NMR spectra were similar to **M4**/**M5**, except for one more methyl signal (δ 4.26, s, 3H), which was correlated with carbonyl carbon signal at δ 174.8 (C-11) in HMBC spectrum (Fig. 3). Thus, the planar structure of **M6** was deduced as 3-butylidene-4,5,6,7-tetrahydro-11-carboxylic-6,7-dihydroxyphthalide-11-methyl ether. Similarly, the relative configuration of C-6 and C-7 in it was deduced to be in *cis* basing on the J values 3.0 Hz of the vicinal signals H-6 and H-7 [5,6], and the absolute configuration was further established as 6*R* and 7*R* on the basis of the positive Cotton effect at 310 nm in the induced CD of **M6** [29] (Fig. 5). It was a pity that the NOE correlation between H-4 and H-8 could not be observed due to the little amount of **M6**. Therefore, the double bond configuration (Δ3,8) is still uncertain. Based on the above spectral data, the structure of **M6** was established as (6*S*,7*R*)-3-butylidene-4,5,6,7-tetrahydro-11-carboxylic-6,7-dihydroxyphthalide-11-methyl ether.

Table 5
^{13}C NMR (δ) for **M10**–**M15** in DMSO (**M11** and **M14** were in MeOD), δ in ppm, J in Hz[a].

No.	M10	M11	M12	M13	M14	M15
1	174.4	171.9	171.1	171.4	171.3	170.4
2	40.8	41.8	40.7	40.9	40.8	40.1
3	171.3	175.8	166.8	165.6	165.5	165.4
4	37.7	38.5	46.2	118.5	119.4	121.4
5	31	32.6	192.4	139.5	139.2	139.4
1′	132.4	143.7	128.2	126.3	127.5	134.7
2′	111.7	116.2	111.5	115.6	110.1	127.6
3′	144.5	158.5	151.9	147.8	150.1	128.9
4′	147.4	114.1	147.5	148.3	148.8	129.6
5′	114.8	130.4	114.9	110.9	111.8	128.9
6′	120.3	120.5	123.7	121.6	121.3	127.6
1-OCH_3		52.6				51.7
3′-OCH_3	55		55.6		55.5	
4′-OCH_3				55.5	55.4	

[a] ^{13}C NMR data (δ) were measured for **M10** at 125 MHz and **M11**–**M15** at 100 MHz.

M7–**M9** had the same molecular formula of $C_{18}H_{24}O_{10}$. The UV and NMR spectra of them were similar to those of senkyunolide I/H ($C_{12}H_{16}O_4$), except for a group of glucuronosyl signals, including six carbon signals at δ 102.6, 73.01, 76.3, 71.8, 75.0, and 169.9 in ^{13}C NMR, as well as five aliphatic proton signals at δ 4.68 (1H, d, J = 7.5 Hz), 3.25 (1H, t, J = 7.5 Hz), 3.42 (1H, t, J = 9 Hz), 3.47 (1H, t, J = 10 Hz) and 3.77 (1H, t, J = 9.5 Hz) in ^{1}H NMR (Table 3). In HMBC spectrum, the proton signal at δ4.68 (in **M7**)/4.48 (in **M9**) of glucuronide moiety were correlative with the carbon signal at δ 70.9/69.2 (C-7), indicating that the glucuronosyl moiety of **M7** and **M9** were linked to C-7 (Fig. 3). The conjugating position of the glucuronosyl group of **M8** was deduced to be at C-6 based on the correlation between C-6 (δ 77.6) and H-1′(4.76) in HMBC spectrum. Thus, the planar structure of **M7** and **M9** were deduced as 3-butylidene-4,5,6,7-tetrahydro-6,7-dihydroxyphthalide-7-*O*-β-D-glucuronide; **M8** were 3-butylidene-4,5,6,7-tetrahydro-6,7-dihydroxy phthalide-6-*O*-β-D-glucuronide. Similarly, the $J_{6,7}$ of **M7**–**M9** were all less than 3.9 Hz, indicating the 6,7-*cis* relative configuration. The NOE for H-4 upon irradiation at H-8 were observed only in **M7** indicating the Δ3,8-*trans* configuration in **M7** and Δ3,8-*cis* configuration in **M8** and **M9** (Fig. 4). To establish the absolute configuration of C-6 and C-7, 2 mg of **M7**–**M9** were hydrolyzed by 50 μL of β-glucuronidase (in 5 mL acetic acid-sodium acetate at 37 °C for 3 h) to obtain their aglycones of **M7a**, **M8a** and **M9a**, respectively. Then **M7a**, **M8a** and **M9a** were solved in DMSO and mixed with $Mo_2(AcO)_4$ to obtain their induced CD spectrum [29] (Fig. 5). All of them showed the positive Cotton effect at 305 nm, indicating the 6*S*- and 7*R*-configuration for **M7**–**M9**. Therefore, their structures were determined as *Z-(6S,7R)*-3-butylidene-4,5,6,7-tetrahydro-6,7-dihydroxyphthalide-7-*O*-β-D-glucuronide (**M7**), *E-(6S,7R)*-3-butylidene-4,5,6,7-tetrahydro-6,7-dihydroxy phthalide-6-*O*-β-D-glucuronide (**M8**), and *E-(6S,7R)*-3-butylidene-4,5,6,7-tetrahydro-6,7-dihydroxyphthalide-7-*O*-β-D-glucuronide (**M9**). The possible planar structures of glucuronided senkyunolide I/H were just deduced on the basis of MS data [28], yet the glucuronided metabolites of senkyunolide I/H were first identified here.

M11 showed the molecular formula of $C_{12}H_{15}NO_4$, as well as UV λ_{max} at 230 nm, 280 nm and a characteristic shoulder peak at 320 nm. There are four aromatic protons at δ 6.59 (1H, d, J = 8 Hz), 6.64 (1H, s), 6.67 (1H, d, J = 7.5 Hz), and 7.06 (1H, t, J = 7.5 Hz) which belong to an ABCD system, one methoxyl signal at δ 3.68 (3H, s), one methylene signal at δ 3.89 (2H, s) and a pair of triplets proton signals of a $-CH_2-CH_2-$ group at δ 2.50 (2H, t, J = 7.5 Hz) and 2.84 (2H, t, J = 7.5 Hz) in ^{1}H NMR spectrum (Table 4). According to the HMBC spectrum, the proton signals of $-CH_2-CH_2-$ group correlated with the aromatic carbon at δ 143.7 (C-1′) and a carbonyl

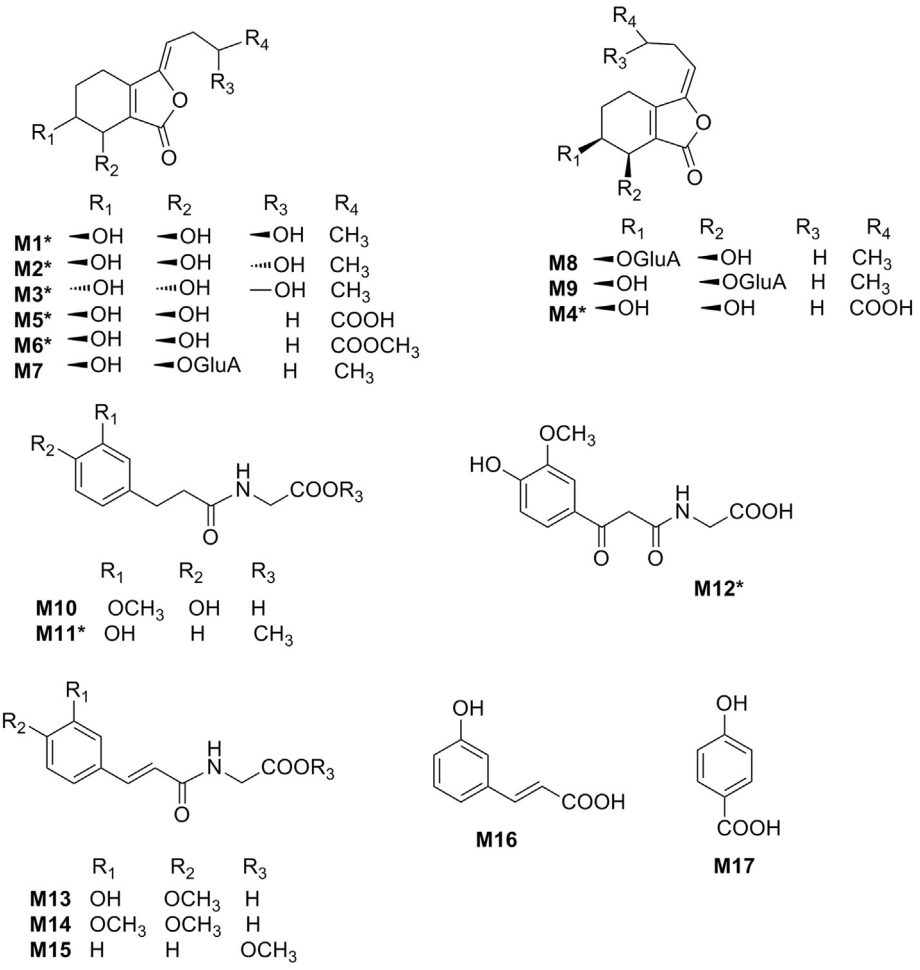

Fig. 2. The structures of **M1**–**M17**. New compounds were marked with *.

carbon at δ 175.8 (C-3), indicated that the $-CH_2-CH_2-$ group was attached between C-1′ and C-3. The methylene proton signal at δ 3.89 (H-2) that correlated to the carboxylic carbon signals at δ 175.8 (C-3) and 171.9 (C-1), suggested that the methylene was attached to C-3 and C-1. Basing on the molecular formula of $C_{12}H_{15}NO_4$ for **M11**, it was deduced to have one carboxylic group

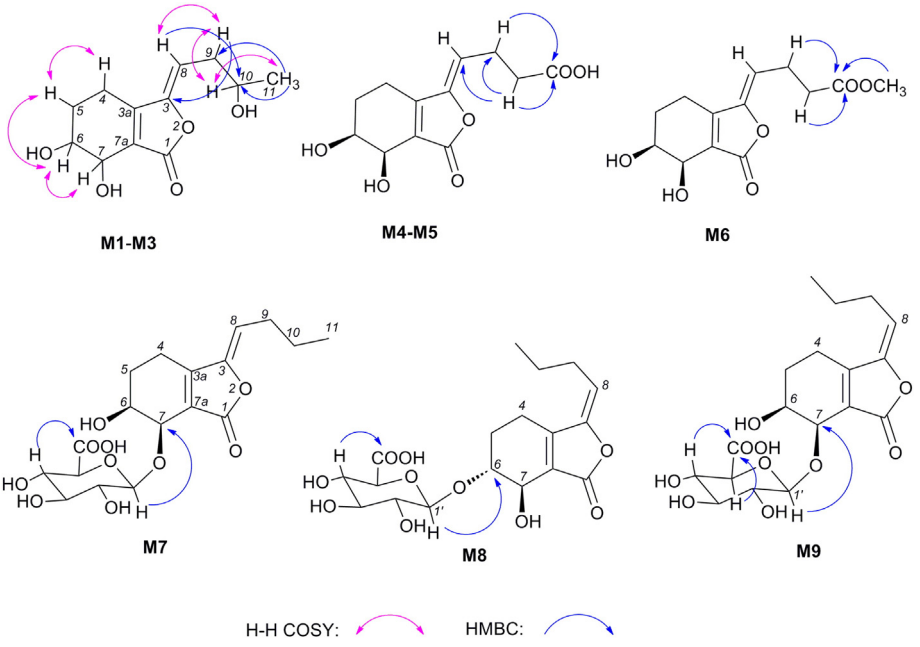

Fig. 3. Key HMBC and ^1H–^1H COSY correlations of **M1**–**M9**.

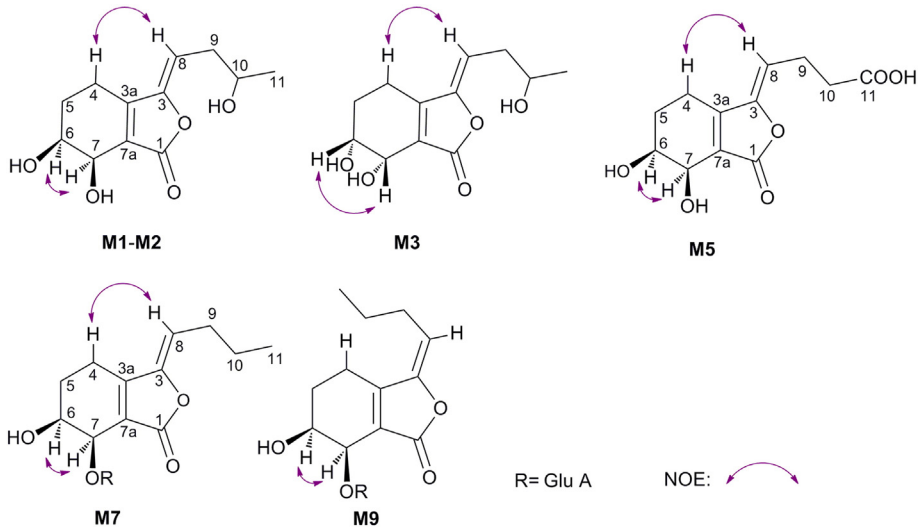

Fig. 4. Key NOESY correlations of **M1**–**M3**, **M5**, **M7** and **M9**.

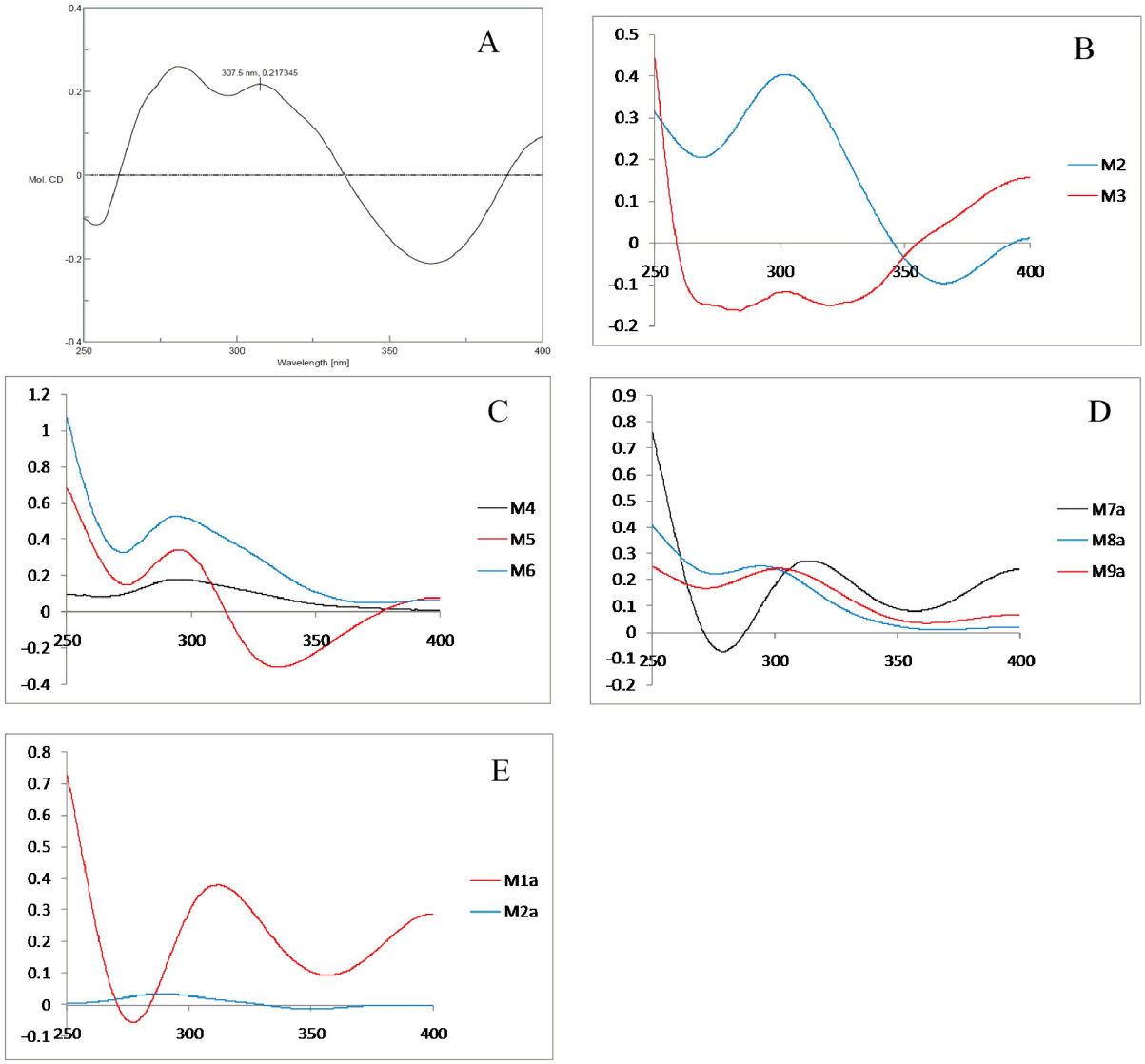

Fig. 5. The CD spectra of *in situ* formed Mo-complexes of **M1** (A), **M2**–**M3** (B), **M4**–**M6** (C), deglucuronidation products of **M7a**–**M9a** (D) and *in situ* formed Rh-complexes of **M1a**–**M2a** (E).

and one acyl amino group. The correlation between methoxyl proton at δ 3.68 (3H, S) and carboxylic carbon at δ 171.9 (C-1) in HMBC spectrum, indicated the existence of a of carboxylic ester in **M11** (Fig. 6). Therefore, the structure of **M11** was determined to be *N*-(3′-hydroxy-4,5-dihydro-cinnamoyl)-glycine-methyl ether.

M12 showed the molecular formula of $C_{12}H_{15}NO_5$. In the ^{1}H NMR spectrum, three aromatic protons at δ 7.52 (1H, d, J = 8.0 Hz), δ 7.45 (1H, s), and δ 6.85 (1H, d, J = 8 Hz) belonging to an ABX system, one methoxyl signal at δ 3.81 (3H, s) and two methylene signals at δ 3.87 (2H, s) and δ 3.79 (2H, d, J = 4 Hz) were observed (Table 4). The structure of **M12** was deduced to possess one carboxylic group and one acylamino group combining the molecular formula information of $C_{12}H_{15}NO_5$. According to the correlations of methylene proton signal at δ 3.87 with carbonyl carbon signal at δ 192.4 (C-5) and carbonyl carbon in acylamino group at δ 166.8 (C-3) in HMBC spectrum, it was suggested that the methylene group was attached to the carbonyl carbon and acylamino carbonyl carbon to form a –CO–CH_2–CO–NH– group. Similar to **M11**, the methylene proton signal at δ 3.79 (H-2) correlated to both carbonyl carbon signals at δ166.8 (C-3) and 171.1 (C-1) in HMBC spectrum, they thus were deduced to form a glycine moiety [32]. The carbon signal at δ 192.4 (C-5) was also correlated to the aromatic proton signals at δ 7.45 (H-2′) and δ 7.52 (H-6′), inferring that C-5 was bonded with the aromatic ring (Fig. 6). Thus, the structure of **M12** was determined to be *N*-(4,5-dihydro-5-carbonyl-feruoyl)-glycine.

M10 and **M13**–**M15** were identified according to their ^{1}H and ^{13}C NMR data (Table 4 and Table 5) as well as their HMBC spectra (Fig. 6). All of them were the glycine conjugate deriving from hydrogenated isoferulic acid (**M10**), isoferulic acid, ferulic acid or caffeic acid (**M13**–**M14**), and cinnamic acid (**M15**), respectively. **M10** could be prepared by N-(carboxyalkyl) dihydoferul amides and used as antioxidants and tyrosinase inhibitors [33]. **M14** existed in the form of metabolites of eugenol methyl ethers in rat [34]. **M15** was prepared for photo crosslinkable cinnamic acid-glycosamino glycan derivative [35].

M16 (*trans*-3-hydroxycinnamoyl acid) and **M17** (4-hydroxybenzoic acid) are two known prototype compounds in CR, which have been isolated from *Salvia bicolor* Desf. growing in Egypt [36] and the roots of *Rheum officinale*, respectively [37]. Their structures were identified by ^{1}H and ^{13}C NMR data, which were consistent with those in references [38,39].

3.2. Discussion

As well known, it is usually difficult and incorrect to determine the exact structures of TCM metabolites only by HPLC-DAD-MS techniques. WZS-miniature pig is not only similar with human in anatomy and physiology, but could also provide much more amounts of samples which will facilitate metabolites isolation and structural elucidation.

Seventeen metabolites (**M1**–**M17**), including 8 new compounds (**M1**–**M6**, **M11**–**M12**), were isolated and identified from the methanol extract of drug-containing urine sample of WZS-miniature pigs after orally administrated CR decoction in this study. **M1**–**M6** were the metabolites derived from the prototype compounds of senkyunolide I/H under the reactions of hydroxylation, methylation, carboxylation, and methylation (Fig. 7). **M11** was deduced as a methylated and glycine conjugated product of 3-hydroxy-cinnamoyl acid (**M16**) after hydrogenated in phase-I metabolic reaction. **M12** was derived from ferulic acid by enoltautomerizing after hydroxylation at 4,5 position of ferulic acid (Fig. 8).

Nine known compounds were first identified as the metabolites of CR, including three isomers of glucuronide conjugates derived from senkyunolide I/H (**M7**, **M8**, **M9**) (Fig. 7), four glycine conjugates deriving from hydrogenated isoferulic acid, isoferulic acid, ferulic acid/caffeic acid, and cinnamic acid (**M10**, **M13**–**M15**), as well as two prototype compounds of 3-hydroxy-cinnamoyl acid (**M16**) and 4-hydroxybenzonic acid (**M17**) (Fig. 8).

It was interesting that glycine conjugated metabolites for phenolic acids in CR were found to be the main metabolic reaction in miniature pigs. Although metabolites of glycine conjugation have been reported in human urine and bile [40,41], this is the first time to report them as the *in vivo* metabolites of constituents of CR.

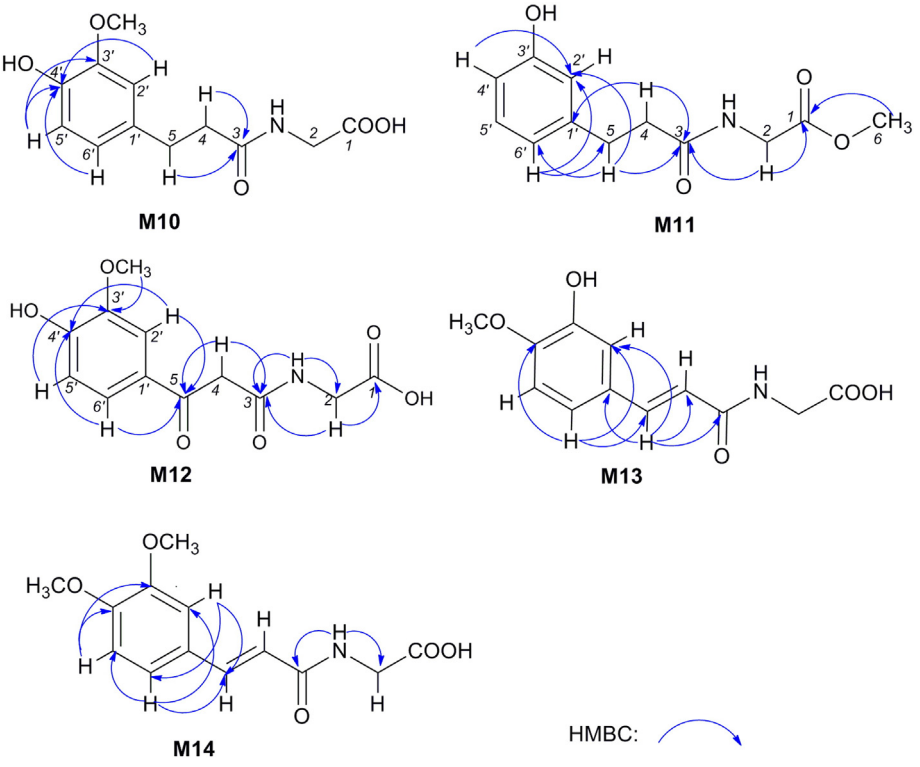

Fig. 6. Key HMBC correlations of **M10**–**M14**.

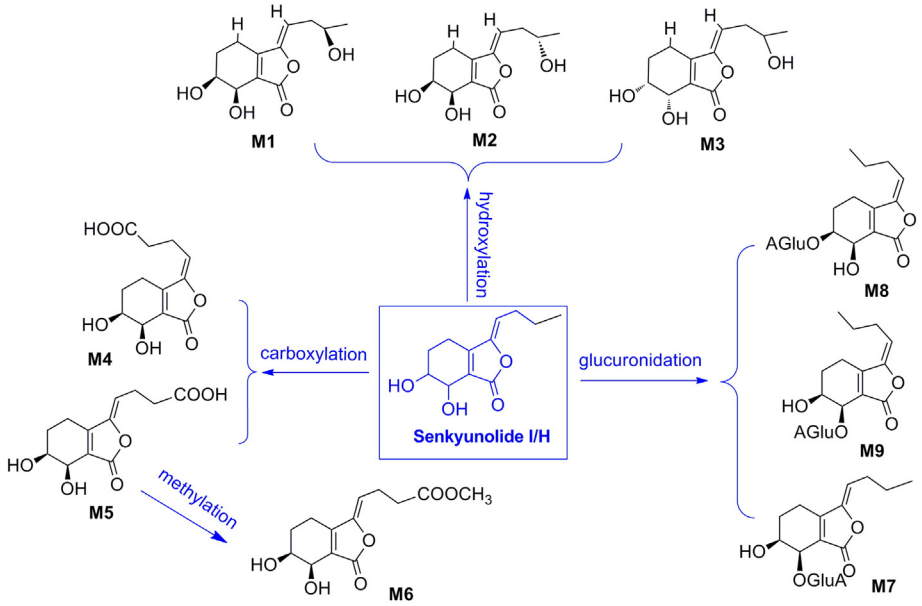

Fig. 7. The proposed metabolic pathways of senkynolide I/H-derived metabolites of CR decoction *in vivo*.

According to the structure skeletons of the identified compounds, 7 original compounds in CR, including two phthalides (senkyunolide I/H) and 5 phenolic acids (ferulic acid, isoferulic acid, caffeic acid, 3-hydroxy-cinnamoyl acid and 4-hydroxybenzonic acid), were deduced to be the absorbed active constituents (Figs. 7 and 8). Ligustilides, commonly recognized as the major constituents in the essential oil of CR, were not detected in the CR decoction, therefore, none ligustilide-derived metabolites were separated from the drug-containing urine sample. Based on the previous studies [42,43], ligustilides are unstable at high temperature or under light exposure and could be rapidly transformed into senkyunolide I/H or their isomers when being decocted for a while. Senkyunolide H/I were reported to possess the activities of anti-migraine [44], reducing hydrogen peroxide-induced oxidative damage in cultured PC12 cells [12] and human liver HepG2 cells [45], and reducing the morphological damage to red blood cells induced by concanavalin A [46]. Ferulic acid and caffeic acid showed the antioxidative [47], anticarcinogenic [48] and antihypertensive [49] activities. Caffeic acid and cinnamic acid could ameliorate glucose metabolism in insulin-resistant mouse hepatocytes [50]. Senkyunolide I/H, and ferulic acid could penetrate blood brain barrier *in vivo* [51,52]. Thus, the phthalides and phenolic acids in CR, and their metabolites *in vivo* should be responsible for the bioactivities of CR decoction. The interactions between the pharmacological and pharmacokinetic activity of phthalide-derived metabolites and phenolic acid-derived metabolites in CR are worth to be further studied.

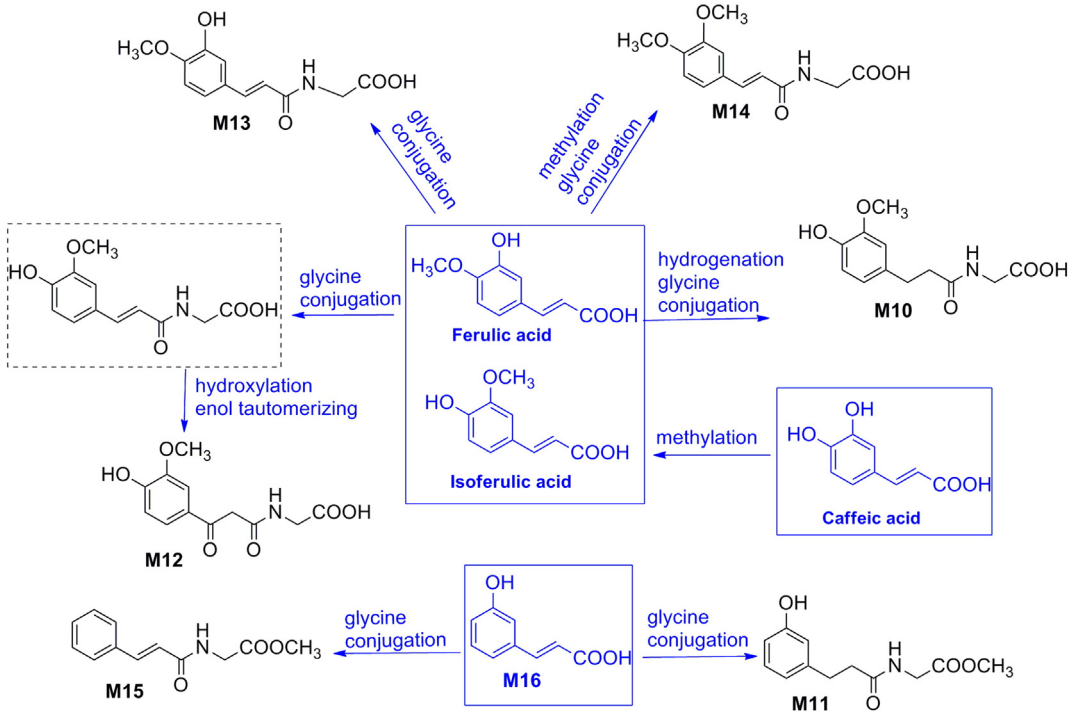

Fig. 8. The proposed metabolic pathways of ferulic acid, isoferulic acid and 3-hydroxycinnamonyl acid (**M16**)-derived metabolites of CR decoction *in vivo*.

4. Conclusions

The absorbed constituents and metabolites of CR decoction *in vivo* were first studied. Seventeen metabolites, including 8 new ones and 9 known ones, were isolated by column chromatography from the drug-containing urine samples of WZS-miniature pigs after oral administration of CR decoction. Their chemical structures were identified by MS, NMR, and CD information. Deducing from the structures of the identified metabolites, 7 original constituents in CR, including 2 phthalides (sankyunolide I/H) and 5 phenolic acids (ferulic acid, isoferulic acid, caffeic acid, 3-hydroxy-cinnamoyl acid and 4-hydroxybenzonic acid) were supposed to be the main absorbed and effective constituents of CR decoction. The results are meaningful for understanding the metabolism profiles of CR decoction *in vivo*, and also provided scientific basis for studying the pharmacokinetic of CR decoction in further.

Acknowledgments

This study was financially supported by Key Program of National Natural Science Foundation of China (Grant No. 30830120), China Postdoctoral Science Foundation (Grant No. 20080430293, Special Grant No. 200902040), and the National Natural Science Foundation of China (Grant No. 81473321).

References

[1] J.W. Ju, J.H. Du, Treatment of migraine with modified chuanxiong powder—a report of 30 cases, J. Tradit. Chin. Med. 15 (1995) 183–184.
[2] K.J. Chen, K. Chen, Ischemic stroke treated with *Ligusticum chuanxiong*, Chin. Med. J. (Engl.) 105 (1992) 870–873.
[3] T.C.T. Or, C.L.H. Yang, A.H.Y. Law, J.C.B. Li, A.S.Y. Lau, Isolation and identification of anti-inflammatory constituents from *Ligusticum chuanxiong* and their underlying mechanisms of action on microglia, Neuropharmacology 60 (2011) 823–831.
[4] L.S. Lim, P. Shen, Y.H. Gong, L.S. Lee, E.L. Yong, Dynamics of progestogenic activity in serum following administration of *Ligusticum chuanxiong*, Life Sci. 79 (2006) 1274–1280.
[5] P.S. Wang, X.L. Gao, Y.X. Wang, Y. Fukuyama, I. Miura, M. Sugawara, Phthalides from the rhizome of *Ligusticum wallichii*, Phytochemistry 23 (1984) 2033–2038.
[6] T. Naito, T. Katsuhara, K. Niitsu, Y. Ikeya, M. Okada, H. Mitsuhashi, Two phthalides from *Ligusticum chuangxiong*, Phytochemistry 31 (1992) 639–642.
[7] T. Naito, Y. Ikeya, M. Okada, H. Mistuhashi, M. Maruno, Two phthalides from *Ligusticum chuanxiong*, Phytochemistry 41 (1996) 233–236.
[8] Y.Q. Xiao, L. Li, X.L. You, M. Taniguchi, K. Baba, Studies on chemical constituents of the rhizomae of *Ligusticum chuanxiong*, China J. Chin. Mater. Med. 27 (2002) 519–522.
[9] X.L. Chang, Y.B. Ma, X.M. Zhang, Z.Y. Jiang, J.J. Chen, Studies on chemical constituents of rhizomes of *Ligusticum chuanxiong*, China J. Chin. Mater. Med. 32 (2007) 1533–1536.
[10] W.X. Wang, M. Gu, X.G. Jiang, Z.L. Gu, P.S. Fan, Studies on chemical constituents of *Ligusticum chuangxiong*, Chin. Tradit. Herb. Drugs 33 (2002) 4–5.
[11] H.B. Lin, F. Chen, Preparative isolation and purification of chuanxiongzine from the medicinal plant *Ligusticum chuanxiong* by high-speed counter-current chromatography, J. Chromatogr. A 1047 (2004) 249–253.
[12] J. Tang, C. Chen, Y. Yu, J.R. Du, W. Yang, C.Y. Wang, Pharmacological activities of Zligustilide and metabolites in rats, J. Sichuan Univ. (Med. Sci. Ed.) 40 (2009) 839–842.
[13] R. Yan, N.L. Ko, S.L. Li, Y.K. Tam, G. Lin, Pharmacokinetics and metabolism of ligustilide, a major bioactive component in Rhizoma Chuanxiong, in the rat, Drug Metab. Dispos. 36 (2008) 400–408.
[14] C.G. Ding, Y.X. Sheng, Y.H. Zhang, J.L. Zhang, G.H. Du, Identification and comparison of metabolites after oral administration of essential oil of *Ligusticum chuanxiong* or its major constituent ligustilide in rats, Planta Med. 74 (2008) 1684.
[15] C.H. Wang, Y.P. Feng, Y.L. Wu, Study on the metabolites of dl-3-n-butylphthalide in rats, Acta Pharm. Sin. 32 (1997) 641–646.
[16] S.H. Peng, T.H. Zhou, Investigation on in vivo metabolism of n-butyl phthalide, Acta Pharm. Sin. 31 (1996) 780–784.
[17] K. Sekiya, Y. Tezuka, K. Tanaka, J.K. Prasain, T. Namba, K. Katayama, et al., Distribution, metabolism and excretion of butylidenephthalide of *Ligustici chuanxiong* rhizoma in hairless mouse after dermal application, J. Ethnopharmacol. 71 (2000) 401–409.
[18] L. Rondini, M.N. Peyrat-Maillard, A. Marsset-Baglieri, C. Berset, Sulfated ferulic acid is the main in vivo metabolite found after short-term ingestion of free ferulic acid in rats, J. Agric. Food Chem. 50 (2002) 3037–3041.
[19] Z. Zhao, Y. Egashira, H. Sanada, Ferulic acid is quickly absorbed from rat stomach as the free form and then conjugated mainly in liver, J. Nutr. 134 (2004) 3083–3088.
[20] Z.C. Zhang, M. Xu, S.F. Sun, X. Qiao, B.R. Wang, J. Han, et al., Metabolic analysis of four phenolic acids in rat by liquid chromatography–tandem mass spectrometry, J. Chromatogr. B 871 (2008) 7–14.
[21] K. Azuma, K. Ippoushi, M. Nakayama, H. Ito, H. Higashio, J. Terao, Absorption of chlorogenic acid and caffeic acid in rats after oral administration, J. Agric. Food Chem. 48 (2000) 5496–5500.
[22] M.Y. Su, T.T. Zhou, M.J. Zhou, The characterization of the metabolites of caffeic acid in rats by LC/MS^n, Chin. J. Mod. Appl. Pharm. 26 (2009) 501–505.
[23] L. Wei, M. Zhou, T. Zhang, W. Hou, L. Wang, J. Xu, Isolation and identification of two glucuronide conjugates in rats metabolized by caffeic acid, Chin. Tradit. Herb. Drugs 41 (2010) 949–952.
[24] X. Chen, S.N. Dong, Studies on the metabolites of tetramethylpyrazine in rabbits, Acta Pharm. Sin. 31 (1996) 617–621.
[25] Y.P. Ye, S.Z. Wang, J. Jiang, Studies on the metabolites of tetramethylpyrazine in human urine, Acta Acad. Med. Sin. 18 (1996) 288–291.
[26] J. Jiang, G.H. Jiang, Y.P. Ye, S.Z. Wang, The metabolism of TMPz in vivo, Acta Acad. Med. Sin. 15 (1993) 79–82.
[27] A.H. Zuo, L. Wang, H.B. Xiao, L.M. Li, Y.H. Liu, J.H. Yi, Identification of the absorbed components and metabolites in rat plasma after oral administration of Rhizoma Chuanxiong decoction by HPLC–ESI–MS/MS, J. Pharm. Biomed. Anal. 56 (2011) 1046–1056.
[28] C.Y. Li, L.W. Qi, P. Li, Correlative analysis of metabolite profiling of Danggui Buxue Tang in rat biological fluids by rapid resolution LC–TOF/MS, J. Pharm. Biomed. Anal. 55 (2011) 146–160.
[29] L. Di Bari, G. Pescitelli, P. Salvadori, Determination of absolute configuration of acyclic 1,2-diols with $[Mo_2(OAc)_4]$, part 2: new structural evidence toward a rationale of the method: what remains of $[Mo_2(OAc)_4]$ in DMSO solution? Chemistry 10 (2004) 1205–1214.
[30] J. Frelek, W.J. Szczepek, $[Rh_2(OCOCF_3)_4]$ as an auxiliary chromophore in chiroptical studies on steroidal alcohols, Tetrahedron Asymmetry 10 (1999) 1507–1520.
[31] M. Gerards, G. Snatzke, Circular dichroism, XCIII determination of the absolute configuration of alcohols, olefins, epoxides, and ethers from the CD of their "in situ" complexes with $[Rh_2(O_2CCF_3)_4]$, Tetrahedron Asymmetry 1 (1990) 221–236.
[32] X. Zhao, D.H. Yang, Q.L. Zhou, F. Xu, L. Zhang, J. Liang, et al., Identification of metabolites in WZS-miniature pig urine after oral administration of Danshen decoction by HPLC coupled with diode array detection with electrospray ionization tandem ion trap and time-of-flight mass spectrometry, Biomed. Chromatogr. 27 (2013) 720–735.
[33] Kato H, Yamaguchi S. Preparation of N-(carboxyalkyl)dihydoferulamides and their uses as antioxidants and tyrosinase inhibitors. JP Patent 2006;2006052150 A 20060223.
[34] E. Solheim, R.R. Scheline, Metabolism of alkenebenzene derivatives in the rat. II. Eugenol and isoeugenol methyl ethers, Xenobiotica 6 (1976) 137–150.
[35] Waki M, Miyamoto K, Motani Y. Cinnamic acid derivatives for photocross linkable cinnamic acid-glycosaminoglycan derivative. EP Patent 1996;1996713859 A2 19960529.
[36] T.A. Ibrahim, Chemical composition and biological activity of extracts from *Salvia bicolor* Desf. growing in Egypt, Molecules 17 (2012) 11315–11334.
[37] L.L. Gao, X.D. Xu, J.S. Yang, Chemical constituents of the roots of *Rheum officinale*, Chem. Nat. Compd. 49 (2013) 603–605.
[38] Z. Yuan, G.Y. Li, Y.M. Zeng, J.H. Wang, Studies on the metabolites of salvianolic acid B, Mod. Chin. Med. 10 (2008) 29–31.
[39] T. Yang, X.M. Cheng, F.S. Yu, G.X. Chou, C.H. Wang, Z.T. Wang, The chemical constituents of *Capparisspinosa* L. fruits, Xibei Yaoxue Zazhi 25 (2010) 260–263.
[40] T.B. Vree, E.W.J. van Ewijk-BenekenKolmer, C.P.W.G. Verwey-van Wissen, Y.A. Hekster, Direct gradient reversed-phase high-performance liquid chromatographic determination of salicylic acid, with the corresponding glycine and glucuronide conjugates in human plasma and urine, J. Chromatogr. 652 (1994) 161–170.
[41] D.M. Lambert, G.K.E. Scriba, J.H. Poupaert, P. Dumont, Anticonvulsant activity of ester- and amide-type lipid conjugates of glycine and N-benzyloxycarbonylglycine, Eur. J. Pharm. Sci. 4 (1996) 159–166.
[42] M. Kobayashi, M. Fujita, H. Mitsuhashi, Studies on the constituents of Umbelliferae plants. XV. Constituents of *Cnidium officinale*: occurrence of pregnenolone, coniferylferulate and hydroxylphthalides, Chem. Pharm. Bull. 35 (1987) 1427–1433.
[43] S.L. Li, R. Yan, Y.K. Tam, G. Lin, Post-harvest alteration of the main chemical ingredients in *Ligusticum chuanxiong* Hort. (Rhizoma Chuanxiong), Chem. Pharm. Bull. 55 (2007) 140–144.
[44] Y. Wang, S. Liang, D.S. Xu, X. Lin, C.Y. He, Y. Feng, Y.L. Hong, Effect and mechanism of senkyunolide I as an anti-migraine compound from *Ligusticum chuanxiong*, J. Pharm. Pharmacol. 2 (2011) 261–266.
[45] H.Y. Qi, S.O. Siu, Y. Chen, Y.F. Han, I.K. Chu, Y. Tong, et al., Senkyunolides reduce hydrogen peroxide-induced oxidative damage in human liver HepG2 cells via induction of hemeoxygenase-1, Chem. Biol. Interact. 183 (2010) 380–389.
[46] M. Hong, Z.B. Dong, Q. Zhu, Effects of ferulic acid, senkyunolide H and senkyunolide I on erythrocytes, Lishizhen Med. Mater. Med. Res. 14 (2003) 738–739.
[47] M.T. Huang, R.C. Smart, C.Q. Wong, A.H. Conney, Inhibitory effect of curcumin, chlorogenic acid, caffeic acid, and ferulic acid on tumor promotion in mouse skin by 12-O-tetradecanoylphorbol-13-acetate, Cancer Res. 48 (1988) 5941–5946.
[48] Y. Kono, K. Kobayashi, S. Tagawa, K. Adachi, A. Ueda, Y. Sawa, et al., Antioxidant activity of polyphenolics in diets. Rate constants of reactions of chlorogenic acid and caffeic acid with reactive species of oxygen and nitrogen, Biochim. Biophys. Acta 1335 (1977) 335–342.
[49] T. Saito, T. Tsuchida, T. Watanabe, Y. Arai, Y. Mitsui, W. Okawa, et al., Effect of coffee bean extract in essential hypertension, Jpn. J. Med. Pharm. Sci. 47 (2002) 67–74.
[50] D.W. Huang, S.C. Shen, Caffeic acid and cinnamic acid ameliorate glucose metabolism via modulating glycogenesis and gluconeogenesis in insulin-resistant mouse hepatocytes, J. Funct. Foods 4 (2012) 358–366.
[51] C.Y. He, S. Wang, Y. Feng, S. Liang, X. Lin, D.S. Xu, K.F. Ruan, Pharmacokinetics, tissue distribution and metabolism of senkyunolideI, a major bioactive componentin *Ligusticum chuanxiong* Hort. (Umbelliferae), J. Ethnopharmacol. 142 (2012) 706–713.
[52] A. Zuo, M. Cheng, L. Wang, H. Xiao, Analysis of chemical constituents of Rhizoma Chuanxiong absorbed in rat brain tissues by UPLC–Q–TOF–MS, Zhongguo Zhongyao Zazhi 37 (2012) 3647–3650.